Supplement of Atmos. Chem. Phys., 21, 8195–8211, 2021
https://doi.org/10.5194/acp-21-8195-2021-supplement

Supplement of

Central role of nitric oxide in ozone production in the upper tropical troposphere over the Atlantic Ocean and western Africa

Ivan Tadic et al.

Correspondence to: Ivan Tadic (i.tadic@mpic.de) and Horst Fischer (horst.fischer@mpic.de)

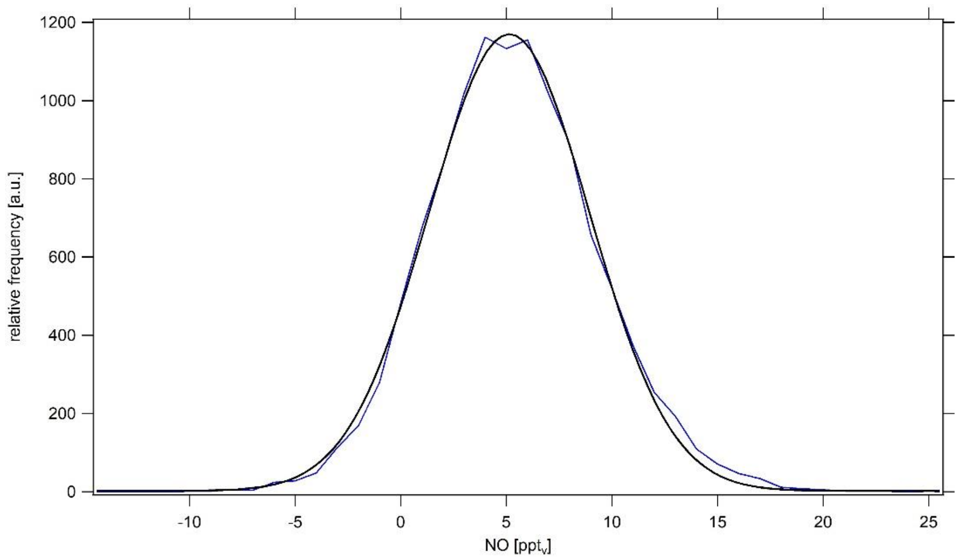

Figure S1: Distribution of in situ NO data (1 s time resolution) obtained during night-time during MF11. Note that the data have not been corrected for the residual instrumental background. The black trace shows a Gaussian fit to the obtained distribution from which the LOD and residual background corrections were retrieved.

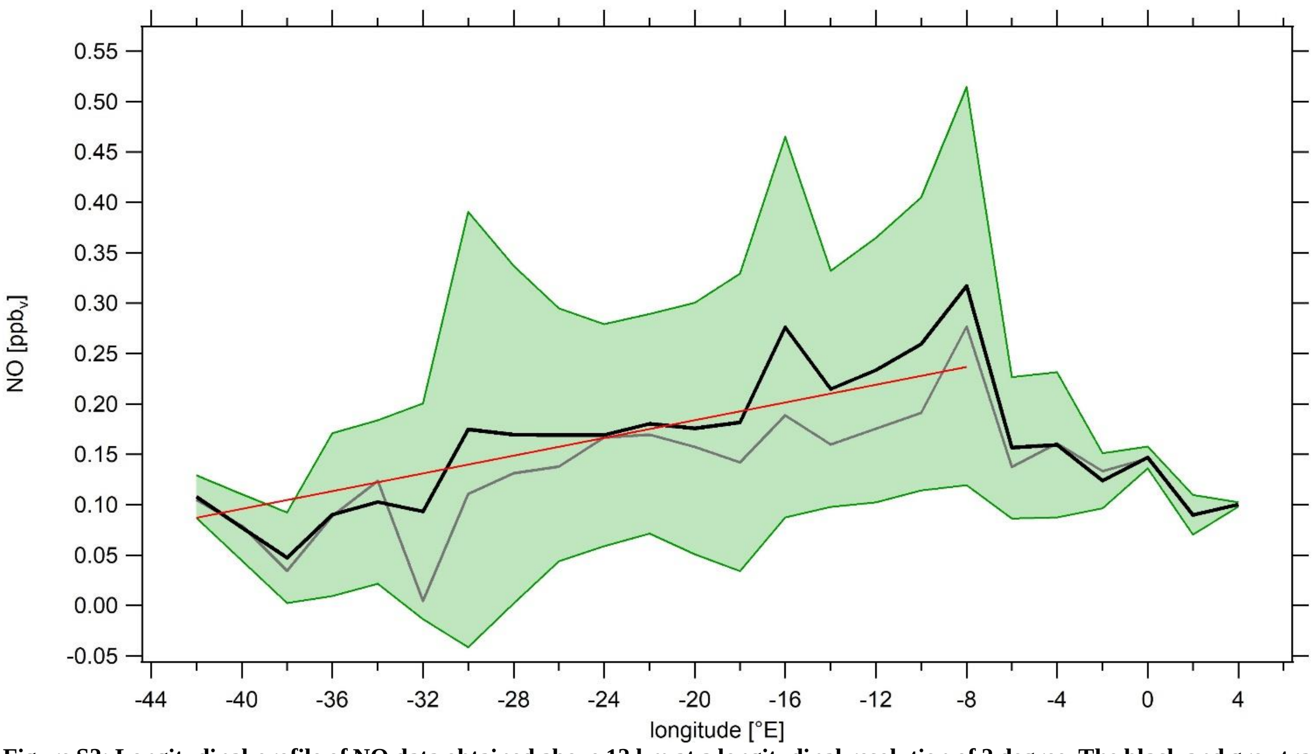

Figure S2: Longitudinal profile of NO data obtained above 12 km at a longitudinal resolution of 2 degree. The black and grey traces represent the average and median longitudinal profile, respectively. The green background represents ±1 standard deviation of the average profile. A linear fit to the averaged data in the interval from -42° E to -8° E (least squares method, weighted by standard deviation of the respective average) yields a longitudinal increase in NO of about 4.4 pptv per degree longitude towards the West African continent. Note that data obtained at latitudes eastbound of -4° N were observed over the European continent.

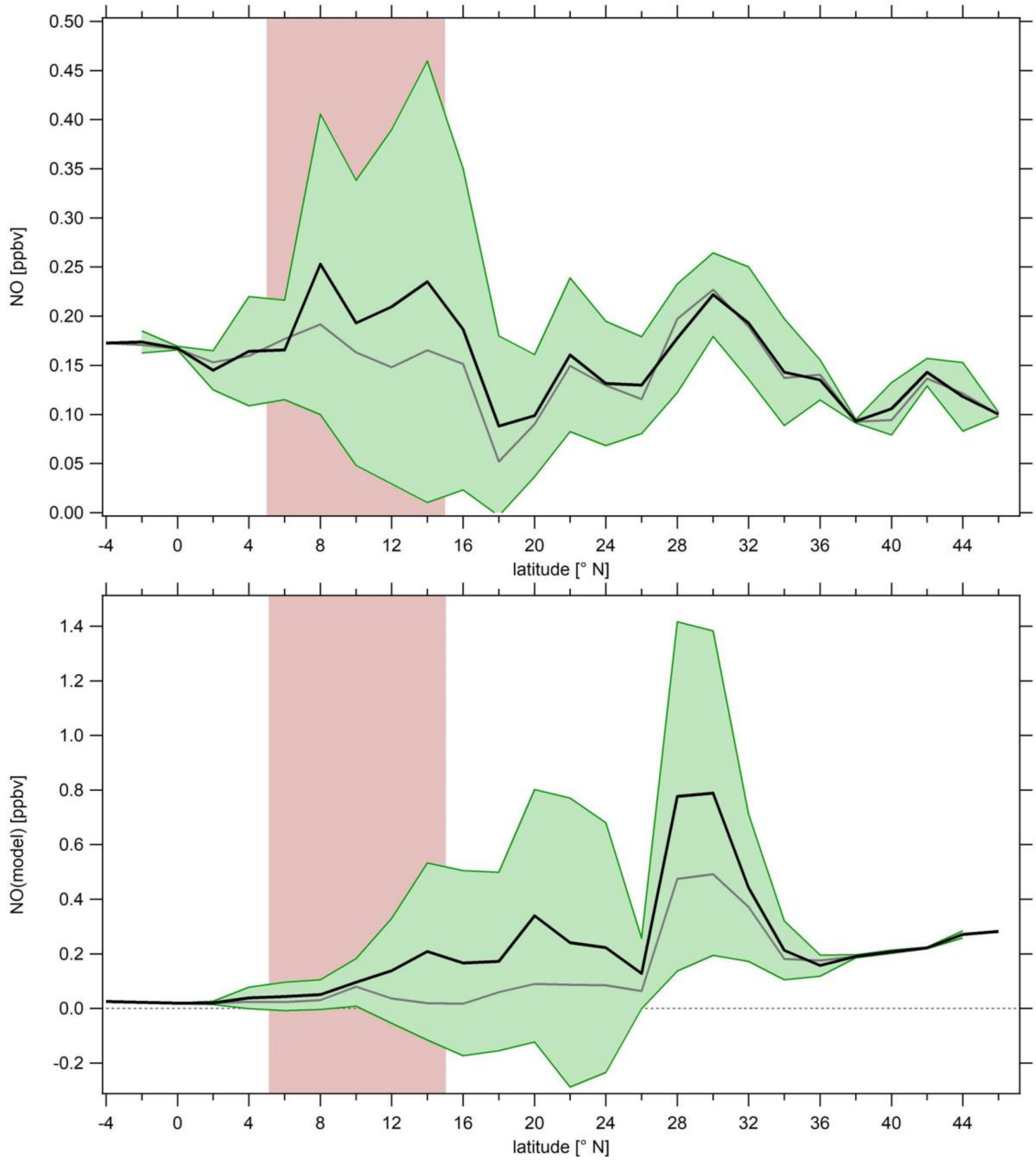

Figure S3: Latitudinal profile of measured (upper plot) and simulated (lower plot) NO data obtained above 12 km at a latitudinal resolution of 2 degree. The black and grey traces represent the average and median latitudinal profile, respectively. The green background represents ± 1 standard deviation of the average profile. The red box in the background indicates the supposable location of the ITCZ during August and September. The profiles were filtered for stratospheric measurements by removing data for which concurrent O_3 is > 100 ppbv.

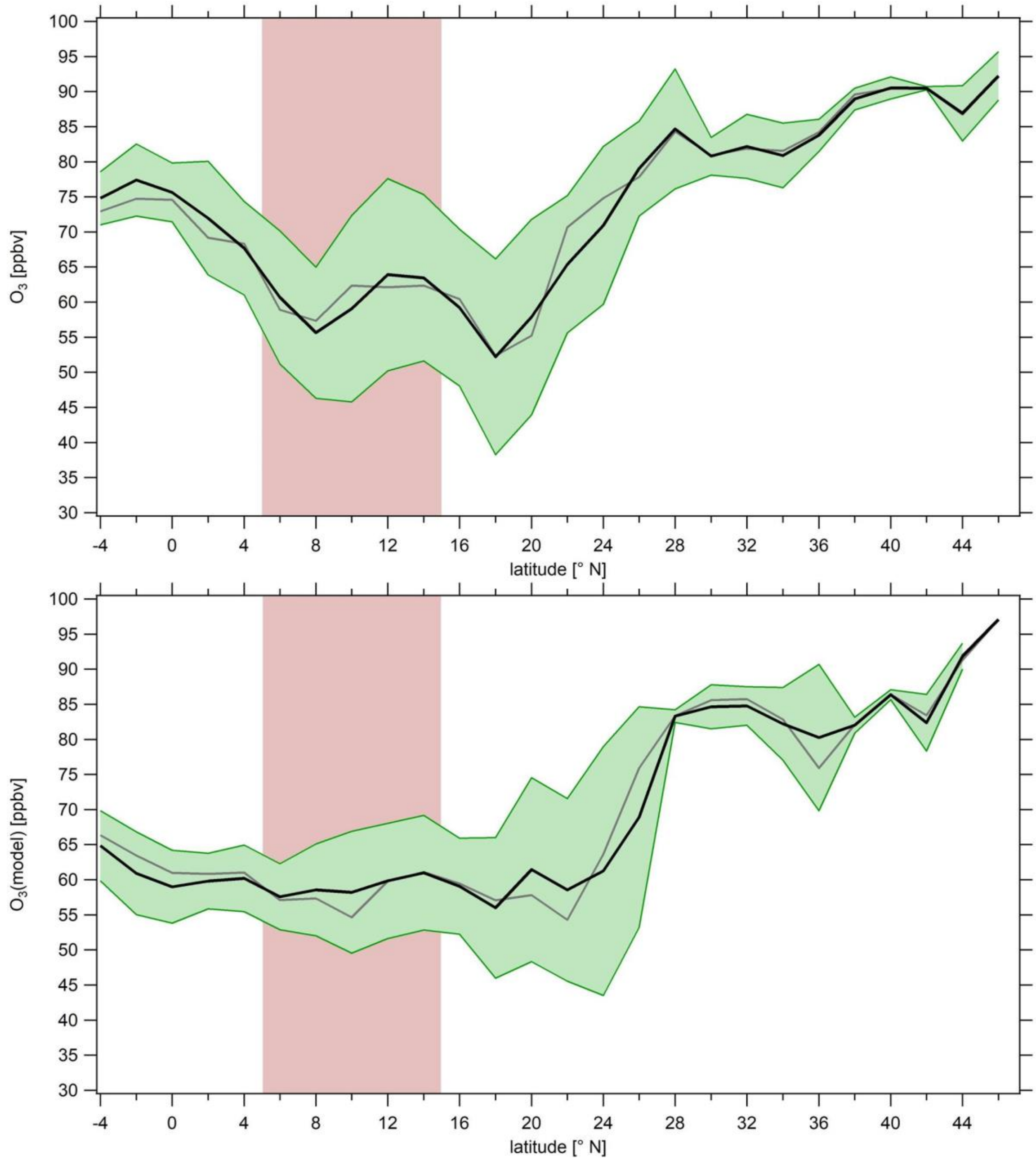

Figure S4: Latitudinal profile of measured (upper plot) and simulated (lower plot) O_3 data obtained above 12 km at a latitudinal resolution of 2 degree. The black and grey traces represent the average and median latitudinal profile, respectively. The green background represents ± 1 standard deviation of the average profile. The red box in the background indicates the supposable location of the ITCZ during August and September. The profiles were filtered for stratospheric measurements by removing data for which concurrent O_3 is > 100 ppbv.

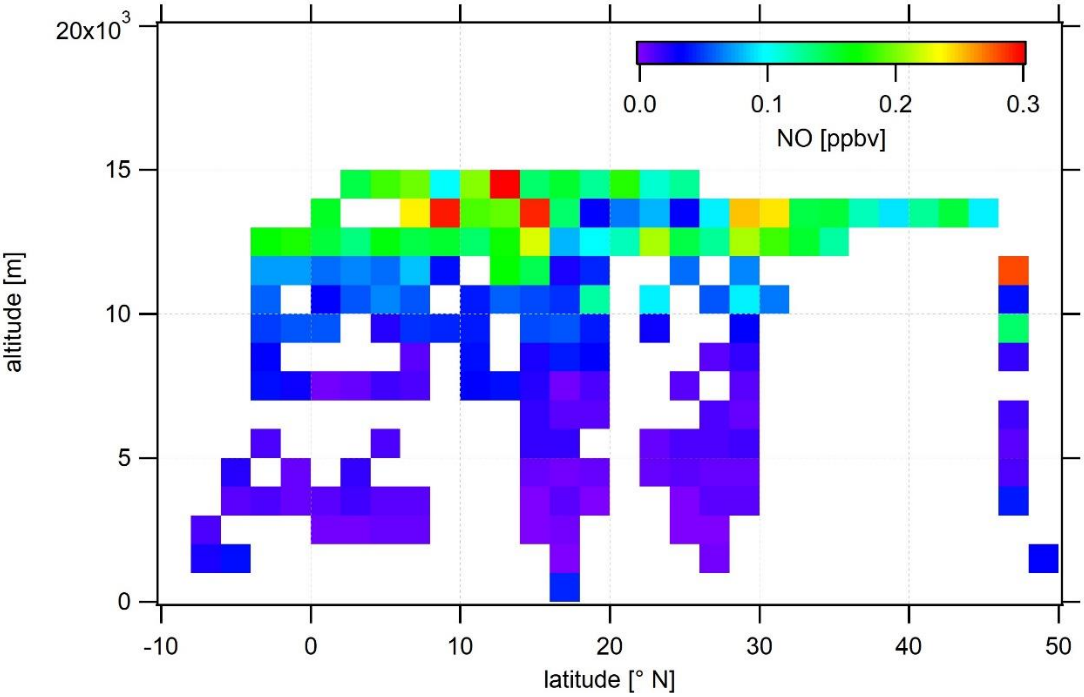

Figure S5: Latitudinal/altitudinal distribution of measured, tropospheric NO obtained during the campaign. The data have been aggregated and averaged over a grid width of 2 degree latitude and 1 km altitude.

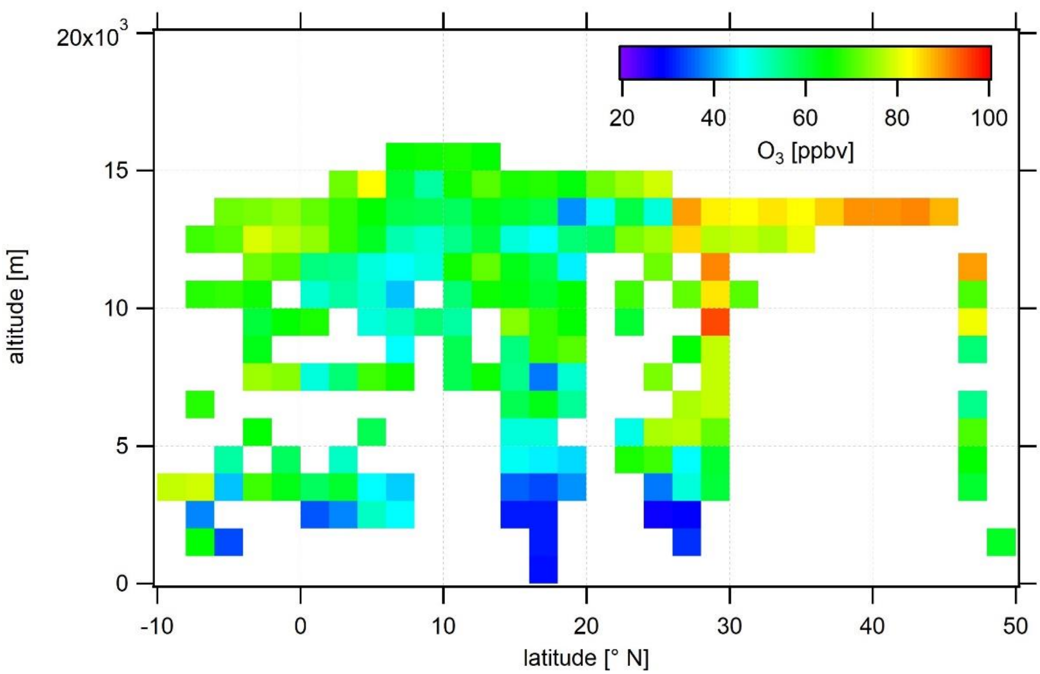

Figure S6: Latitudinal/altitudinal distribution of measured, tropospheric O_3 obtained during the campaign. The data have been aggregated and averaged over a grid width of degree latitude and 1 km altitude.

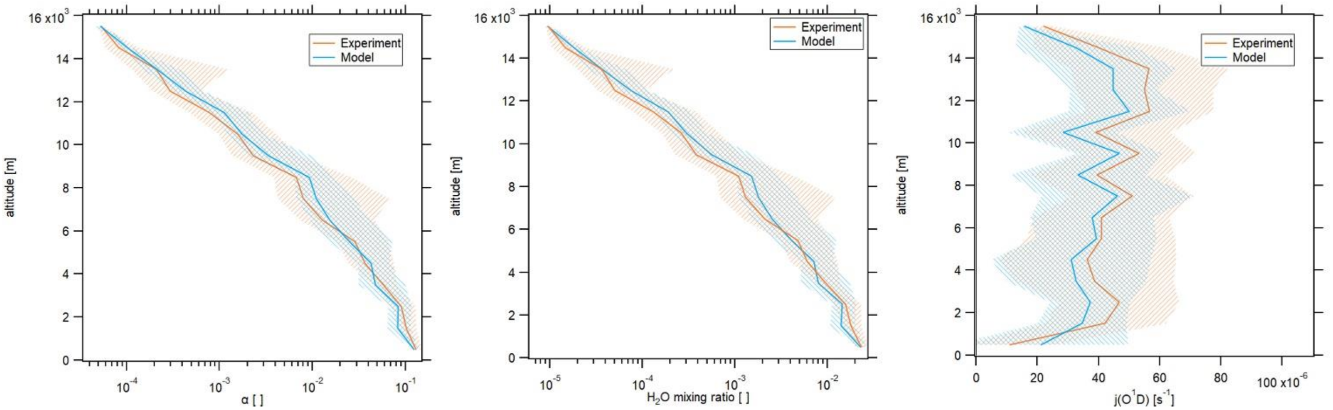

Figure S7: Vertical, tropospheric profile of α calculated based on measured and simulated data during CAFE-Africa (left graph). Vertical, tropospheric profile of H_2O mixing ratios calculated based on measured and simulated data during CAFE-Africa (middle graph). Vertical, tropospheric profile of $j(O^1D)$ (measured and simulated) obtained during CAFE-Africa (right graph). The orange and blue traces represent measured and simulated results, respectively.

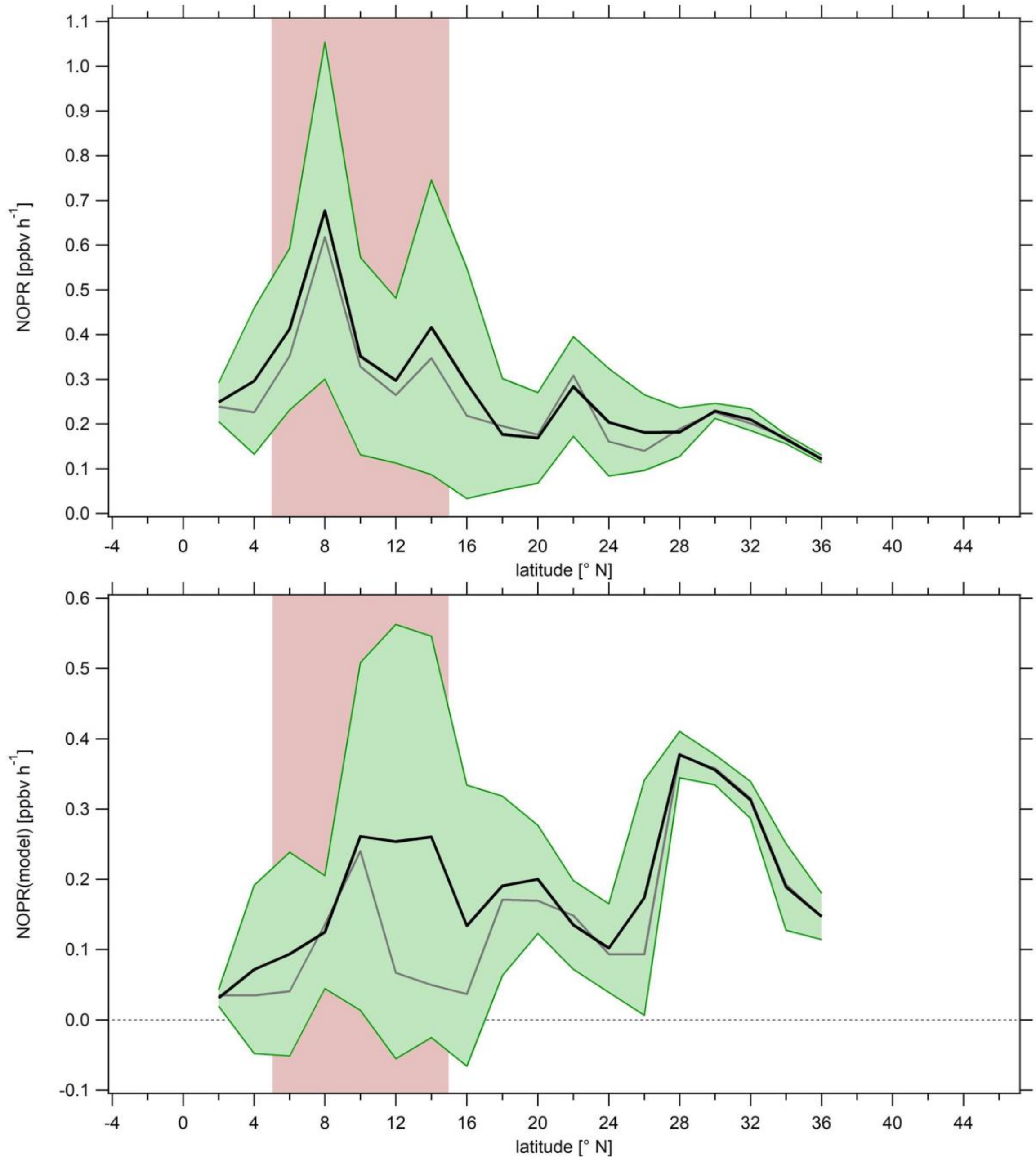

Figure S8: Latitudinal profile of NOPRs derived from measured (upper plot) and simulated (lower plot) data above 12 km at a latitudinal resolution of 2 degree. The black and grey traces represent the average and median latitudinal profile, respectively. The green background represents ±1 standard deviation of the average profile. The red box in the background indicates the supposable location of the ITCZ during August and September. The profiles were filtered for stratospheric measurements by removing data for which concurrent O_3 is > 100 ppbv.

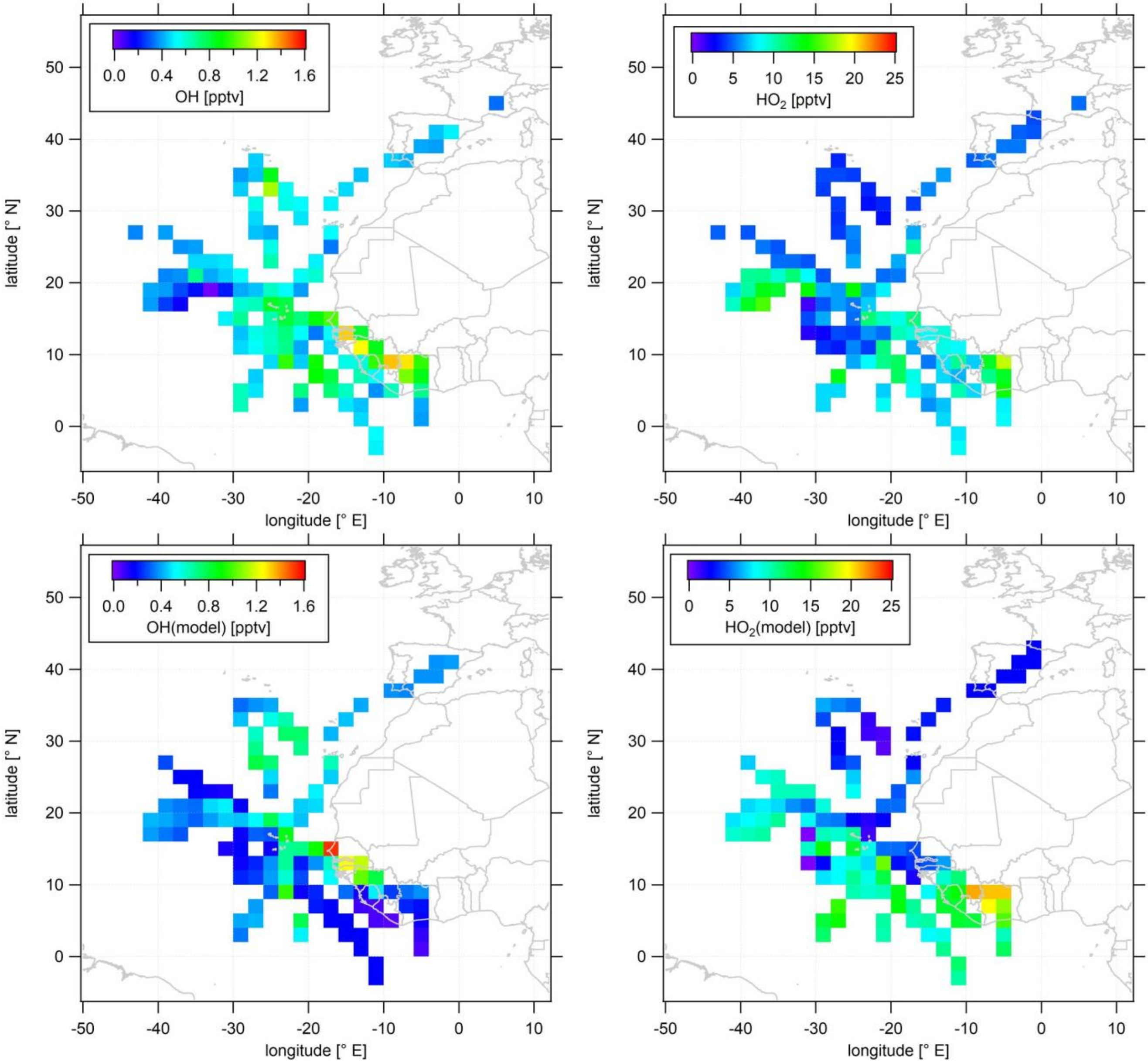

Figure S9: Color-coded spatial, tropospheric distributions of measured and simulated OH and HO_2 above 12 km during CAFE-Africa. The upper graphics show the measurements, the lower graphics show the simulations. Note that the figures are filtered for stratospheric measurements by removing data points for which concurrent O_3 is > 100 ppbv.

Table ST1: Overview of the scientific measurement flights performed during CAFE-Africa. EDMO is the international civil aviation organization (ICAO) code of the airport of the DLR facility at South Germany, GVAC the ICAO code of the airport on Sal and DGAA the ICAO code of the airport of Accra (Ghana).

Flight number	Date of the flight	Purpose/objective of the flight	Flight route
MF03	07 August 2018	ferry flight to Sal (Cape Verde Islands)	EDMO → GVAC
MF04	10 August 2018	flight south / biomass burning plume	GVAC → GVAC
MF05	12 August 2018	flight south / aged biomass burning plume	GVAC → GVAC
MF06	15 August 2018	flight north / stratospheric influence	GVAC → GVAC
MF07	17 August 2018	stack flight #1	GVAC → GVAC
MF08	19 August 2018	stack flight #2	GVAC → GVAC
MF09	22 August 2018	flight over West Africa	GVAC → DGAA
MF10	24 August 2018	flight northwest / aged biomass burning plume	GVAC → GVAC
MF11	26 August 2018	stack flight #3	GVAC → GVAC
MF12	29 August 2018	flight over the ITCZ	GVAC → GVAC
MF13	31 August 2018	flight over the ITCZ	GVAC → GVAC
MF14	02 September 2018	convective outflow of hurricane “Florence”	GVAC → GVAC
MF15	04 September 2018	flight over West Africa	GVAC → GVAC
MF16	07 September 2018	ferry flight to Oberpfaffenhofen (Germany)	GVAC → EDMO

Table ST2: List of peroxy radicals (with less than four carbon atoms) which were used to estimate RO_2 (in analogy to Tadic et al., 2020).

Species
HO_2
CH_3O_2
C_2H_5O2
$C_2H_5CO_3$
CH_3CO_3
C3DIALO2 ($C_3H_3O_4$)
CH_3CHOHO_2
$CH_3COCH_2O_2$
CH_3COCO_3
$CHOCOCH_2O_2$
$CO_2H_3CO_3$
$HCOCH_2CO_3$
$HCOCH_2O_2$
$HCOCO_3$
$HCOCOHCO_3$
$HOC_2H_4CO_3$
$HOCH_2CH_2O_2$
$HOCH_2CO_3$
$HOCH_2COCH_2O_2$
$HOCH_2O_2$
$CH_3CHO_2CH_2OH$
IC3H7O2 (isopropylperoxy radical)
NC3H7O2 (propylperoxy radical)
$NCCH_2O_2$
$NO_3CH_2CO_3$
$CH_3CHO_2CH_2ONO_2$

Table ST3: Number of data points in each NO mixing ratio bin. Note that the data coverage of the simulation is larger than that of the measurement due to gaps in the observational data.

NO mixing ratio bin	measurement	simulation
0 pptv ≤ NO < 25 pptv	140	226
25 pptv ≤ NO < 50 pptv	54	70
50 pptv ≤ NO < 75 pptv	36	40
75 pptv ≤ NO < 100 pptv	23	60
100 pptv ≤ NO < 125 pptv	50	38
125 pptv ≤ NO < 150 pptv	44	24
150 pptv ≤ NO < 175 pptv	28	7
175 pptv ≤ NO < 200 pptv	30	7
200 pptv ≤ NO < 225 pptv	21	3
225 pptv ≤ NO < 250 pptv	15	7
250 pptv ≤ NO < 275 pptv	11	3
275 pptv ≤ NO < 300 pptv	12	5
300 pptv ≤ NO < 325 pptv	11	5
325 pptv ≤ NO < 350 pptv	3	3
350 pptv ≤ NO < 375 pptv	2	6
375 pptv ≤ NO < 400 pptv	3	2
400 pptv ≤ NO < 425 pptv	1	1
425 pptv ≤ NO < 450 pptv	5	2
450 pptv ≤ NO < 475 pptv	1	3
475 pptv ≤ NO < 500 pptv	1	3